Plastic Collapse Assessment Procedure for Vessels with Deep Local Thin Area Subjected to Internal Pressure

N. Mukaimachi
JGC Corporation
Shinji Konosu
Ibaraki University

Abstract
There are numerous cases in which the external surfaces of vessels such as towers, piping and storage tanks are partially corroded under their insulation. Some considerations on the plastic condition of cylinders with a local thin area have been reported, but a simplified evaluation procedure has not been established for the case in which a cylinder is simultaneously subjected to internal pressure and external bending moment due to earthquake, etc. Recently, the Ibaraki FFS rule has been presented, but the limitation on flaw depth (a) in the Ibaraki FFS rule is less than 0.7 (=a/t) of the original wall thickness (t). The effective cross section for the reference stress solution used to predict the plastic collapsed loads was investigated by nonlinear FEA. For the case in which a flaw depth to thickness ratio is large ($a/t \le 0.70-0.95$), the reference stress solution which decreases the effective cross section as a function of the flaw depth ratio was proposed.

Keywords: fitness for service (FFS), collapse limit, p-M method, local thin area, effective cross section, deep flaw, reference stress

1. Introduction

There are numerous cases in which the external surfaces of vessels such as towers, piping and storage tanks are partially corroded under their insulation. Some considerations on the plastic condition of cylinders with a local thin area (LTA) have been reported [1-3], but a simplified evaluation procedure has not been established for the case in which a cylinder is simultaneously subjected to internal pressure and external bending moment due to earthquake, etc. Then, the Ibaraki FFS rule was newly developed [4]. The Ibaraki FFS rule assessment procedure based on the p-M method is a simple evaluation procedure, which can be readily used to assess a vessel with an LTA simultaneously subjected to internal pressure and bending moment due to earthquake, etc [5, 6]. The limitation with respect to flaw depth (a) has been set as within 0.7 (=a/t) of the original wall thickness (t) in the Ibaraki FFS rule. So far, however, very little work has been done on the limitation with respect to a flaw depth for the reference stress. This paper proposes the reference stress solution for deep flaw depth.

2. Ibaraki FFS rule assessment procedure

The procedures described in the Ibaraki FFS rule [4] based on the p-M (internal pressure ratio

and external bending moment ratio) method [5,6] were used to predict the collapsed loads for cylinders with an LTA subjected to combined internal pressure and bending moment. The method is based on the plastic collapse condition in which the reference stress of a crack-like flaw instead of a volumetric flaw reaches the flow stress of the material.

For an external longitudinal surface flaw, the following reference stress is defined [5].

$$\sigma_{ref} = \frac{\frac{1}{3} g\sigma_b + \sqrt{\left(\frac{1}{3} g\sigma_b\right)^2 + (1-\alpha)^2 M_s{}^2 \sigma_m{}^2}}{(1-\alpha)^2} \qquad (1)$$

For a thick cylinder, the average circumferential stress due to pressure is given as

$$\sigma_m = \frac{4 - 6\tau + 3\tau^2}{2\tau(2-\tau)} p \qquad (2)$$

The plastic collapse condition is decided when the reference stress meets the flow stress of the material, as given in the following equation.

$$\sigma_{ref} = \sigma_f \qquad (3)$$

The plastic collapse pressure, p^L for an external longitudinal flaw under pure internal pressure is derived from Eqs. (1)-(3) as follows;

$$p^L = \frac{2\tau(2-\tau)}{4 - 6\tau + 3\tau^2} \frac{1-\alpha}{M_s} \sigma_f \qquad (4)$$

Equation (4) as the collapse pressure is adopted in the Ibaraki FFS rule. The relative rectangular flaw depth, α proposed by Willoughby and Davey [7] is used. The flaw is assumed to be rectangular, in an effective cross section of $t(l+2t)$ as shown in Fig. 1. The effective flaw depth to thickness ratio is given by

$$\alpha = \frac{a_{eff}}{t} = \frac{la}{t(l+2t)} \qquad (5)$$

In the Ibaraki FFS rule, a flaw is assumed to be semi-elliptical. Then the area of a rectangular surface flaw set to equal the area of a semi-elliptical surface crack, is given by the following equation:

$$l = \frac{\pi c_L}{2} \qquad (6)$$

It substitutes Eq. (6) for Eq. (5), and then the following equation is derived. a_{eff} is the rectangular flaw depth equivalent to a semi-elliptical flaw depth.

$$\alpha = \frac{a_{eff}}{t} = \frac{\pi a c_L}{t(\pi c_L + 4t)} \qquad (7)$$

3. FEA model

In order to confirm the applicable limit of the Ibaraki FFS rule, the collapse load is calculated by nonlinear finite element analysis (FEA) applied to some vessels with an external deep LTA. Table 1 shows the geometric parameters and materials of the cylinders. Material nonlinearity is considered as well as geometrical nonlinearity. The FEA software, ABAQUS [8], is used. Three-dimensional shell elements (S4R) are applied. FEA models "A" and "B" were analyzed by using the experimentally obtained true stress-strain relation shown in Fig. 2. The material was typical Japanese carbon steel (STPG370) as shown in Table 2. Young's Modulus, yield stress and Poisson's ratio are 203GPa, 326MPa and 0.3, respectively.

FEA model "C" was analyzed as an elastic-perfectly plastic material which has the yield stress of 326MPa in order to determine a lower bound to the limit load. And Young's Modulus and Poisson's ratio are 203GPa and 0.3, respectively.

LTA sizes are $l \times 2c_\theta$ and LTA thicknesses of models "A" and "B" are constant (t_{lg} =2.5mm). FEA models adopted are 1/4 models due to the symmetry. The thick flat head is set to one end of the cylinder. Pressure is loaded to the inside of the cylinder and the flat head. The configurations of vessels with an LTA and finite element mesh for the models of A, C and B are shown in Figs. 3 and 4, respectively. The determination of the collapse load (TES: twice elastic slope load) is decided according to ASME [9] as given in the following equation.

$$\phi = tan^{-1}(2\tan\theta_{el}) \qquad (8)$$

where θ_{el} is the angle that the regression line makes with the ordinate, and the angle ϕ decides the collapse limit line. The collapse load is determined as the intersection of the collapse limit line with the load-displacement or load-strain curve.

4. FEA results

The load-strain curves obtained at the center of an LTA are shown in Figs. 5, 6 and 7. These strains are circumferential logarithmic strain at the center of the external surface of the LTA. The collapse loads (TES loads) decided from these figures by using the method proposed by ASME are listed as p_TES in Table 3. Symbols △ and ○ in Fig. 7 denote the plastic collapsed loads estimated by Konosu et al. [5] and Kiefner et al. [10], respectively. Mises stress on the outside surface around an LTA of Model A at near TES load is shown in Fig. 8. From the figure, Mises stress over almost the entire region of LTA exceeds the yield stress at around TES load. Then it

is found that LTA meets the collapsed condition at TES load. For $a/t \geqq 0.8$, the changes in value of p_TES for models A and B are small because the thin thicknesses of these LTAs are restrained tightly by greater thickness around the LTA. The ratio of collapsed load by FEM to that by Eq. (4) based on measured yield stress is shown in Table 3 and Fig. 9. If the ratio exceeds 1.0, Eq. (4) provides the collapsed load, p^L, on the conservative side. From Fig. 9, the Ibaraki FFS rule using Eq. (4) estimates collapsed loads conservatively where $a/t \leqq 0.75$, but it estimates collapsed loads less-conservatively where $a/t > 0.75$.

5. Proposition of modified a_{eff}

When a crack becomes deep, the definition of Eq. (5) for the effective cross section $t(l+2t)$ may not be appropriate. As shown in Fig. 10, for a deep crack depth, it is reasonable to consider that the effective cross section becomes narrower than the value of $t(l+2t)$. Therefore a modified Eq. (9) is proposed here. The effective cross section of $t(l+kt)$ is assumed and the value of k is assumed to vary with the value of a/t. As $k=2$ can be set for a shallow crack depth conforming to the idea proposed by Willoughby and Davey [7], the value of k is derived so as to satisfy the condition that p^L coincides with p_TES. The values of k obtained are listed in Table 4 and Fig. 11. And the curve fit for the value of k in the range of $a/t=0.8$ to 0.95 of Model C results in the following equation.

$$\alpha = \frac{a_{eff}}{t} = \frac{\pi a c_L}{t(\pi c_L + 2kt)} \qquad (9)$$

where

$$k = \begin{cases} 2 & : a/t \leq 0.76 \quad (10a) \\ -154.6\left(\frac{a}{t}\right)^3 + 456.3\left(\frac{a}{t}\right)^2 - 450.0\left(\frac{a}{t}\right) + 148.3 & : 0.76 < a/t < 0.95 \quad (10b) \end{cases}$$

6. Comparison between the collapsed load by modified a_{eff} and FEM

The collapsed loads are calculated by Eqs. (4) and (9) where the flow stress is assumed to be measured yield stress. The ratio of the collapsed loads by FEM to that by Eqs. (4) and (9) are shown in Table 5 and Fig. 12. For comparison purposes, the results of Eq.(7) (namely k=2) are incorporated into Fig. 12. As is evident from Fig.12, Eq. (9) provides the collapsed loads conservatively.

7. Discussion

The plastic collapse pressure p_0^L for a cylinder without a flaw under pure internal pressure is expressed from Eq. (2) as follows;

$$p_0^L = \frac{2\tau(2-\tau)}{4-6\tau+3\tau^2}\sigma_f \qquad (11)$$

The plastic collapse pressure, p^L, for a cylinder with an external longitudinal flaw under pure internal pressure to p_0^L abovementioned ratio is given from Eqs. (4) and (11) as follows;

$$p^L / p_0^L = p^L / \left[\frac{2\tau(2-\tau)}{4-6\tau+3\tau^2}\sigma_f\right] = \frac{1-\alpha}{M_s} \qquad (12)$$

Whereas Kiefner et al. [10] presented p^L / p_0^L for surface flaw due to pressure as follows;

$$p^L / p_0^L = p^L / \left[\frac{2\tau(2-\tau)}{4-6\tau+3\tau^2}\sigma_f\right] = \frac{1}{M_s^{Kiefner}} \qquad (13)$$

$$M_s^{Kiefner} = \frac{1-\frac{a}{t}\frac{1}{M_t}}{1-\frac{a}{t}} \qquad (14)$$

Fig. 13 gives the dependence of the value of a/t on p^L / p_0^L for λ=1.0. Also shown for comparison purposes are p_TES / P_0^L by FEA results plotted. The Ibaraki FFS rule using Eq. (10a) should be restricted as $a/t \leqq 0.7$, but the limitation may be mitigated until $a/t \leqq 0.95$ if Eq. (10b) proposed here is adopted. The plastic collapsed loads given by Eq. (10a) for λ=1.0 by Konosu et al.[5] are evaluated more conservatively than that of Kiefner's empirical Eq. (13) derived from high strength steels (API 5L X52-X100) until $a/t \leqq 0.8$. From Fig.7 the strains equivalent to the plastic collapsed loads predicted by Eq. (13) by Kiefner et al. are as large as 5.7-7.1% in $0.85 \leqq a/t \leqq 0.90$.

Experimental test data for a deep flaw conducted by the Special Post-construction Committee of Ibaraki Prefecture [11] and Eq.(10b) presented here are compared. The material used in the test was a typical Japanese carbon steel (STPG370) as shown in Table 2 and Fig.2. The flaw configuration and geometrical parameters of the test cylinder are shown in Fig.14 and Table 6. Fig. 15 shows the load-strain curve at the center of LTA under pure internal pressure and the collapsed load (TES load) decided by using the method proposed by ASME is 4.20MPa. Fig. 16

gives the dependence of the value of a/t on p^L / p_0^L for λ=1.4. Also shown for comparison purposes are p_TES / P_0^L by FEA and the experimental results plotted. As hardness was distributed through the thickness of the test cylinder and some scatter of the material strength is generally inevitable [6], the specified minimum yield stress was adopted in the Ibaraki FFS rule, reflecting the uncertainties in material strength. Therefore, the TES load obtained from the experiment was normalized by the plastic collapse pressure for a cylinder without a flaw based on the specified minimum yield strength as flow stress. The results of the FEM and experiment test are in a good agreement with the value predicted by Eq. (10b) proposed here.

8. Conclusion

The effective cross section for the reference stress solution used to predict plastic collapsed loads was investigated by nonlinear FEA. Where a flaw depth ratio (a/t) is large, the following reference stress solution resulting from a decrease in the effective cross section as a function of the flaw depth ratio has been proposed, resulting in the mitigation of limitation with respect to the flaw depth ratio.

$$p^L = \frac{2\tau(2-\tau)}{4-6\tau+3\tau^2}\frac{1-\alpha}{M_s}\sigma_f$$

where,

$$\alpha = \frac{a_{eff}}{t} = \frac{\pi a c_L}{t(\pi c_L + 2kt)}$$

$$k = \begin{cases} 2 & : a/t \le 0.76 \\ -154.6\left(\frac{a}{t}\right)^3 + 456.3\left(\frac{a}{t}\right)^2 - 450.0\left(\frac{a}{t}\right) + 148.3 & : 0.76 < a/t < 0.95 \end{cases}$$

Acknowledgements

The authors are grateful to the members of the Specialized Committee for Safety of Ibaraki Prefecture. The authors would also like to thank Mr. S. Kanamaru, Senior Engineer of JGC Corporation, for his assistance during the preparation of this paper.

Nomenclature

a : Flaw depth

a_{eff} : Rectangular flaw depth equivalent to a half elliptical flaw depth

$2c_L$: Longitudinal flaw length of a half elliptical flaw

$2c_\theta$: Circumferential flaw length

LTA : Local thin area

$g = 1 - 20\left(\frac{a}{2c}\right)^{0.75}\alpha^3$: Modified factor for bending stress

$l = 2c$: Flaw length of a rectangular flaw

$M_t = \sqrt{1 + 0.317\lambda^2}$: Bulging factor for a through-wall flaw

$M_s = \frac{1}{1 - \frac{a}{t} + \frac{a}{t}\frac{1}{M_t(a)}}$: Bulging factor for a part-through flaw

$M_s^{Kiefner} = \frac{1 - \frac{a}{t}\frac{1}{M_t}}{1 - \frac{a}{t}}$: Surface correction factor by Kiefner et al. [10]

p : Internal pressure

$p_0^L = \frac{2\tau(2-\tau)}{4 - 6\tau + 3\tau^2}\sigma_f$: The plastic collapse internal pressure for a cylinder without a flaw under pure pressure

$p^L = \frac{2\tau(2-\tau)}{4 - 6\tau + 3\tau^2}\frac{1-\alpha}{M_s}\sigma_f$: Plastic collapse internal pressure for an external surface flaw under pure pressure

p_max : Plastic instability pressure determined as the maximum load

p_TES : Collapse pressure determined under the twice-elastic slope method

$R_o = D_o / 2$: Outer radius of cylinder

$R_i = D_i / 2$: Inner radius of cylinder

TES : Twice-elastic slope

t : Wall thickness

$t_{lg}(= t - a)$: Ligament thickness of a cylinder

$\alpha = \frac{a_{eff}}{t} = \frac{\pi a c_L}{t(\pi c_L + 4t)}$: Relative rectangular flaw depth

$\phi = tan^{-1}(2\,tan\,\theta_{el})$: Gradient of collapse limit line

$\lambda = \frac{1.818 c_L}{\sqrt{R_i t}}$: Shell parameter for a through-wall flaw

$\lambda_a = \frac{1.428 c_L}{\sqrt{R_i a}}$: Shell parameter for a part-through flaw

θ_{el} : Initial gradient of load versus displacement or strain curve per FEA

σ_f : Flow stress of the material

σ_{ys}^{mean} : Measured yield stress

σ_{ys}^{min} : Specified minimum yield stress

σ_{ref} : Reference stress

σ_m : Tensile stress component

σ_b : Bending stress component

$\tau = \frac{t}{R_o}$: Ratio of thickness to outer radius of a cylinder

References

[1] BS7910, 2005, "Guide to methods for assessing the acceptability of flaws in metallic structures".

[2] API 579-1/ASME FFS-1, 2007, "Fitness-For-Service".

[3] FITNET, 2005, "Fitness for service procedure".

[4] Ibaraki FFS rule, 2006, "Assessment Standard for Externally Corroded Pressure Equipment", Ibaraki Prefecture of Japan.

[5] Konosu S. and Mukaimachi N., 2006, "Plastic Collapse Assessment Procedure for Vessel with Local Thin Area Simultaneously Subjected to Internal Pressure and External Bending Moment", Proceeding of ASME PVP2006-93496; ASME J. Pressure Vessel Technology, Vol.130, Feb. 2008.

[6] Konosu S., Kano M., Mukaimachi N., Komura H. and Takada H., 2007, "Plastic Collapse Load for Vessel with External Flaw Simultaneously Subjected to Internal Pressure and External Bending Moment –Experimental and FEA Results-", Proceeding of ASME PVP2007-26410; ASME J. Pressure Vessel Technology, to be published.

[7] Willoughby A. A. and Davey T. G., 1989, “Plastic Collapse in Part-Wall Flaws in Plates”, ASTM STP 1020, pp.390-409.
[8] ABAQUS, Version 6.6.2, DASSAULT SYSTEMES.
[9] ASME, 2004, Boiler and Pressure Vessel Code Section VIII, Div.2.
[10] Kiefner J. F., Maxey W. A., Eiber R. J., Dufly A. R., 1973, “Failure Stress Levels of Flaws in Pressurized Cylinders”, ASTM STP536, pp.461-481
[11] Special Post-construction Committee of Ibaraki Prefecture, 2008, “Substantive Tests for Assessment Procedure in Ibaraki FFS rule” (in Japanese)

Table 1 Geometric parameters of the cylinders for FEA models

Model		a/t	t_{lg} mm	a mm	t mm	l mm	$2c_L$ mm	$2c_\theta$ mm	D_m mm	D_m/t	λ	Material property
A	A-1	0.5	2.5	2.50	5.00	90	114.6	90	483.3	96.7	3.01	Material−1
	A-2	0.7		5.83	8.33					58.0	2.34	
	A-3	0.8		10.0	12.5					38.7	1.92	
	A-4	0.85		14.2	16.7					29.0	1.67	
	A-5	0.9		22.5	25.0					19.3	1.38	
	A-6	0.95		47.5	50.0					9.7	1.00	
B	B-1	0.5	2.5	2.50	5.00	300	382.0	838	1600	320	5.50	Material−1
	B-2	0.7		5.83	8.33					192	4.26	
	B-3	0.8		10.0	12.5					128	3.49	
	B-4	0.85		14.2	16.7					96	3.02	
	B-5	0.9		22.5	25.0					64	2.47	
	B-6	0.95		47.5	50.0					32	1.76	
C	C-1	0.7	15.0	35.00	50.00	90	114.6	90	483.3	9.7	1.00	Material−2
	C-2	0.75	12.5	37.50								
	C-3	0.8	10.0	40.00								
	C-4	0.85	7.5	42.50								
	C-5	0.9	5.0	45.00								
	C-6	0.95	2.5	47.50								

Note: Stress strain curves of Material−1and Material−2 are shown in Fig.2.

Table 2 Mechanical properties of STPG370 (Material-1) [6]

Young's modulus (GPa)	203
Specified yield stress, σ_{ys}^{min} (MPa)	≧215
Specified tensile stress, σ_{uts}^{min} (MPa)	≧370
Test temperature	RT
Measured yield stress, σ_{ys}^{mean} (MPa)	326
Measured tensile stress, σ_{uts}^{mean} (MPa)	483

Table 3 FEA results and the collapsed load p^L by Eqs.(4) and (7)

Model		a/t	p_TES (MPa)	p_max (MPa)	p^L (MPa)	p_TES/p^L
A	A-1	0.5	4.75	7.757	2.75	1.73
	A-2	0.7	5.23	11.97	3.46	1.51
	A-3	0.8	5.5	17.32	5.05	1.09
	A-4	0.85	5.64	22.62	7.20	0.78
	A-5	0.9	5.81	30.8	12.8	0.45
	A-6	0.95	5.91	36.47	37.4	0.16
B	B-1	0.5	1.27	2.484	0.675	1.88
	B-2	0.7	1.29	3.654	0.671	1.93
	B-3	0.8	1.31	5.029	0.808	1.62
	B-4	0.85	1.32	5.924	1.022	1.29
	B-5	0.9	1.32	7.068	1.631	0.81
	B-6	0.95	1.32	8.172	4.782	0.28
C	C-1	0.7	57.1		45.66	1.25
	C-2	0.75	48.2		44.00	1.10
	C-3	0.8	35.5		42.34	0.84
	C-4	0.85	23.2		40.69	0.57
	C-5	0.9	13.1		39.05	0.34
	C-6	0.95	5.86		37.41	0.16

Table 4 The value of k which is decided as $p^L = p\_TES$

Model		a/t	k
A	A-1	0.5	2
	A-2	0.7	2
	A-3	0.8	2
	A-4	0.85	1.13
	A-5	0.9	0.405
	A-6	0.95	0.0726
B	B-1	0.5	2
	B-2	0.7	2
	B-3	0.8	2
	B-4	0.85	2
	B-5	0.9	1.25
	B-6	0.95	0.192
C	C-1	0.7	2
	C-2	0.75	2
	C-3	0.8	1.2
	C-4	0.85	0.52
	C-5	0.9	0.205
	C-6	0.95	0.071

Table 5 The collapsed load p^L (k=Eq.(10)) estimated by Eq.(9)

Model		a/t	p^L (k=Eq.(10))	p_TES/p^L (k=Eq.(10))
A	A-1	0.5	2.75	1.73
	A-2	0.7	3.46	1.51
	A-3	0.8	4.22	1.30
	A-4	0.85	4.28	1.32
	A-5	0.9	4.48	1.30
	A-6	0.95	5.51	1.07
B	B-1	0.5	0.67	1.88
	B-2	0.7	0.67	1.92
	B-3	0.8	0.73	1.78
	B-4	0.85	0.76	1.74
	B-5	0.9	0.82	1.61
	B-6	0.95	0.99	1.34
C	C-1	0.7	45.66	1.25
	C-2	0.75	44.00	1.10
	C-3	0.8	35.20	1.01
	C-4	0.85	23.45	0.99
	C-5	0.9	12.92	1.01
	C-6	0.95	5.51	1.06

Table 6 Geometric parameters of the experimental test [11]

Model	a/t	t_{lg}	a	t	$2c_L$	$2c_\theta$	D_o	D_o/t	λ	Material
v_IdsP	0.82	0.98	4.45	5.43	30.35	30.16	165.5	30.5	1.35	STPG370

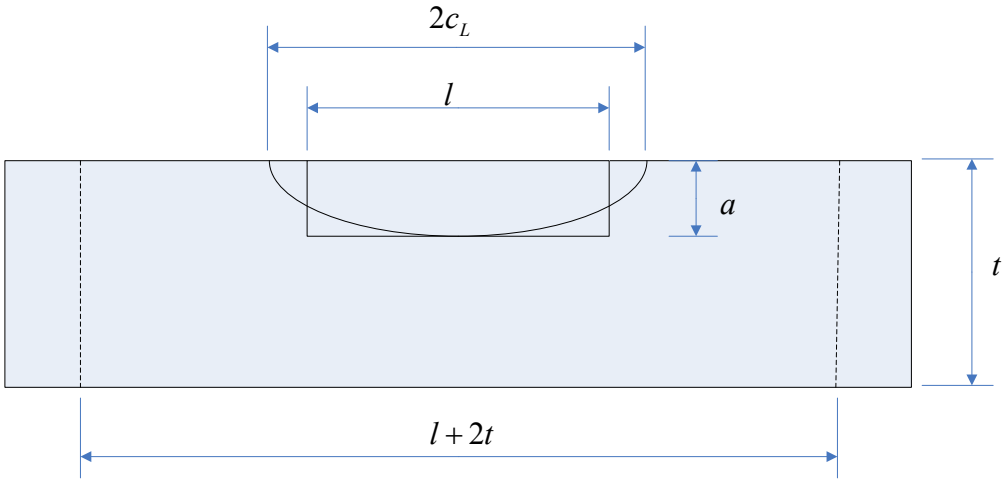

Fig. 1 Effective flaw area and effective cross section

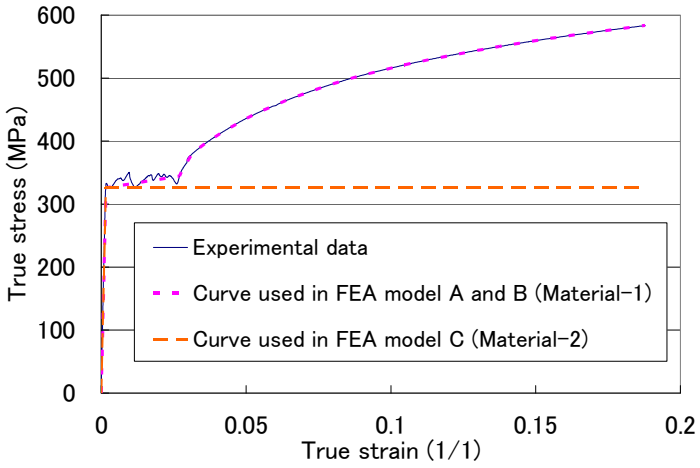

Fig. 2 True stress strain curve for FEA models

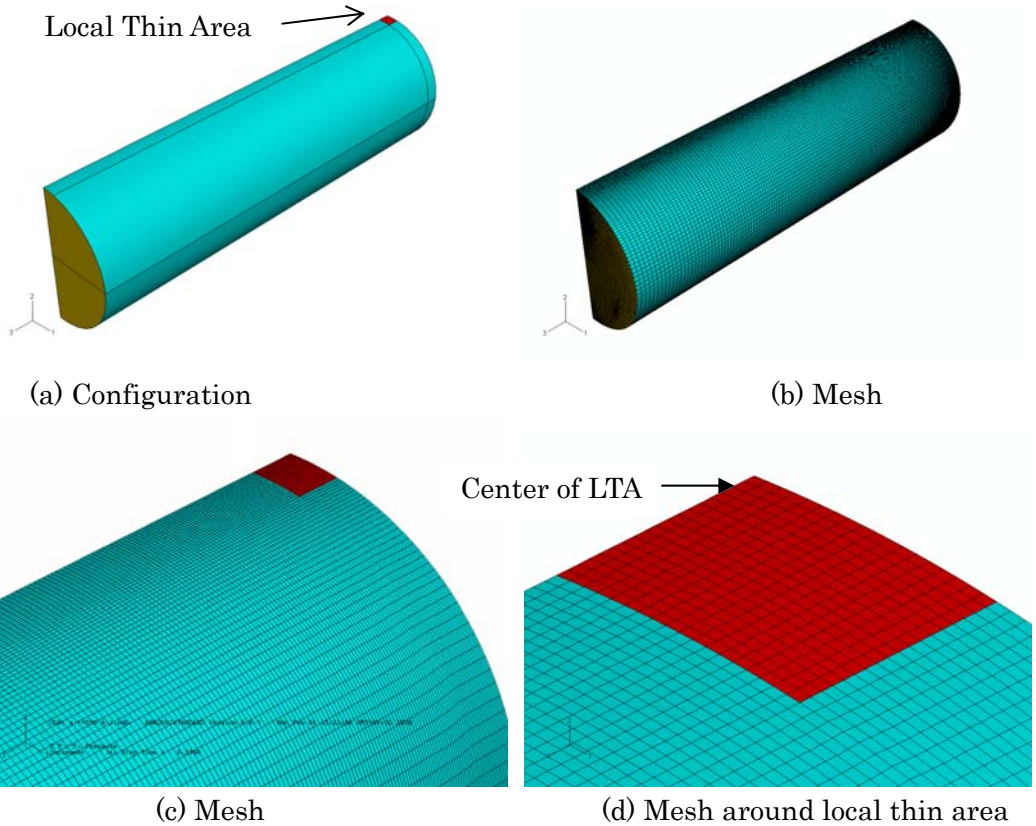

(a) Configuration (b) Mesh

(c) Mesh (d) Mesh around local thin area

Fig. 3 Configuration and FE mesh of models A and C

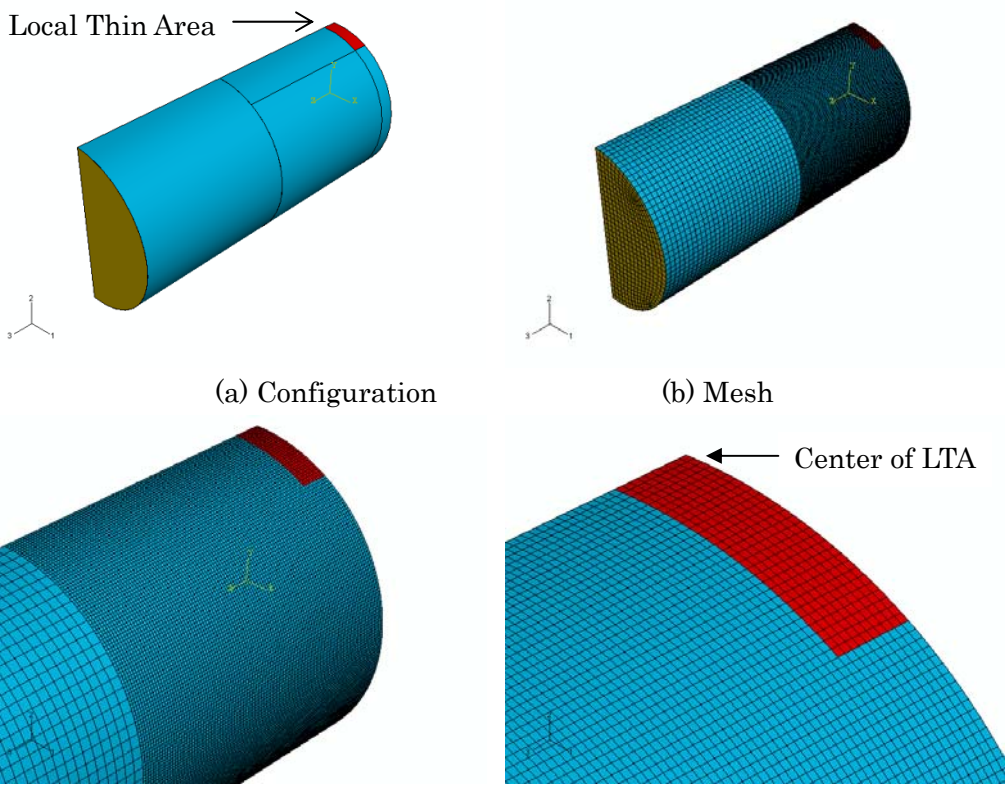

(a) Configuration (b) Mesh

(c) Mesh (d) Mesh around local thin area

Fig. 4 Configuration and FE mesh of model B

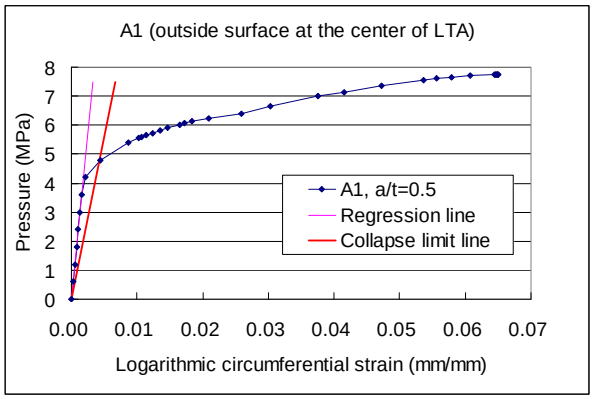

(a) A-1

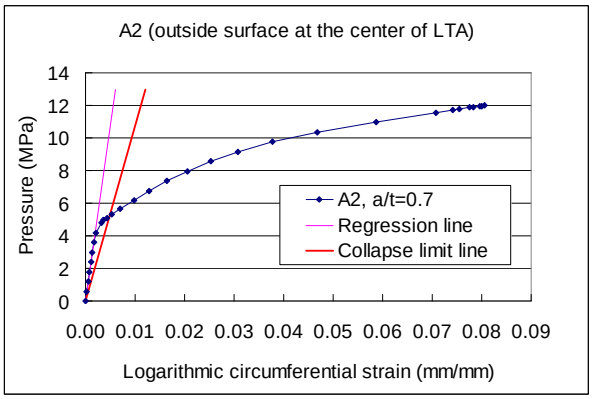

(b) A-2

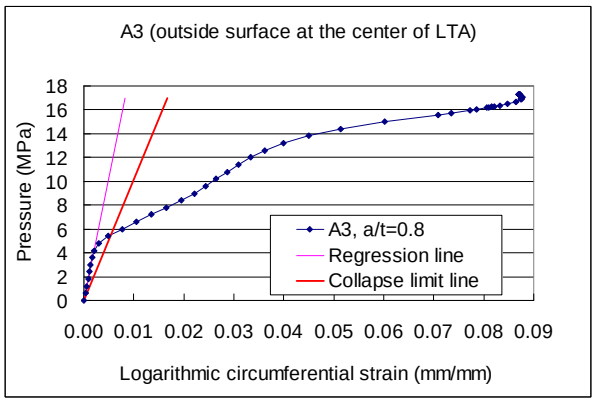

(c) A-3

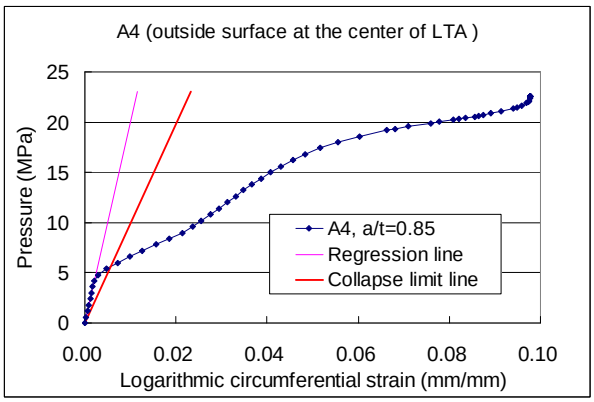

(d) A-4

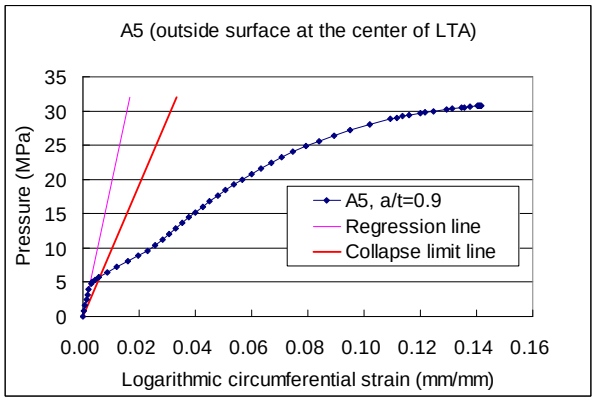

(e) A-5

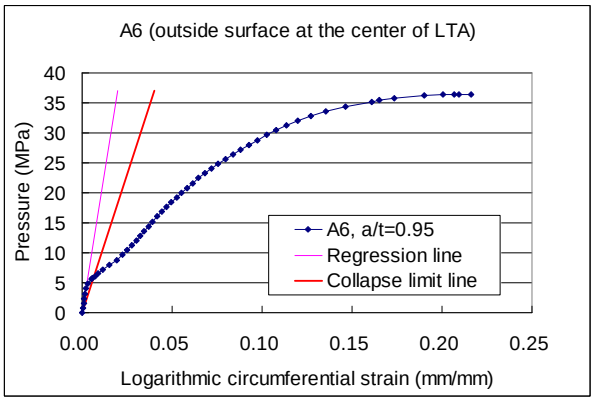

(f) A-6

Fig. 5 Strain history at center of LTA of FE model A

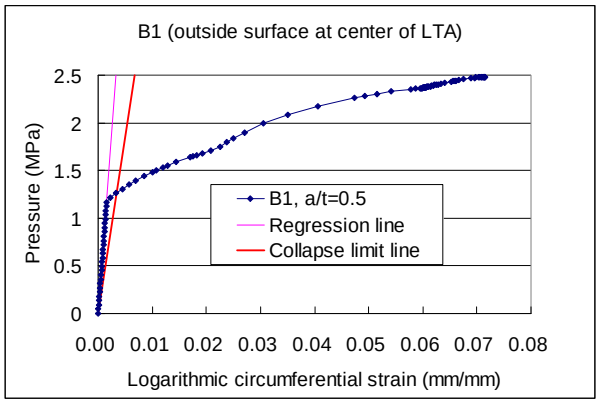

(a) B-1

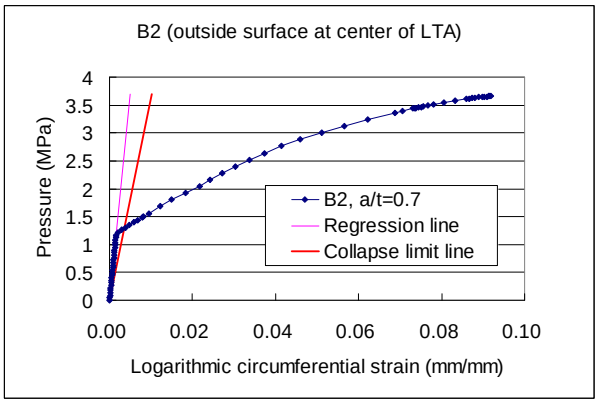

(b) B-2

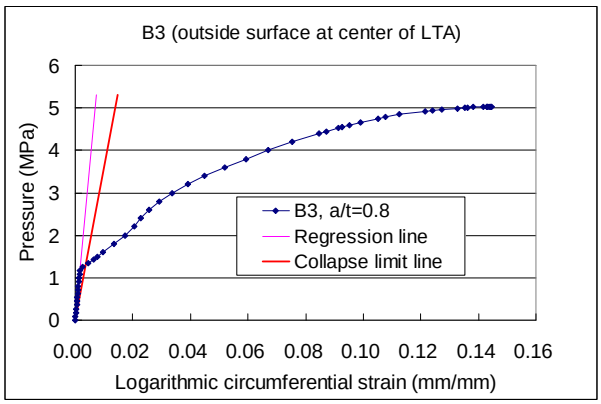

(c) B-3

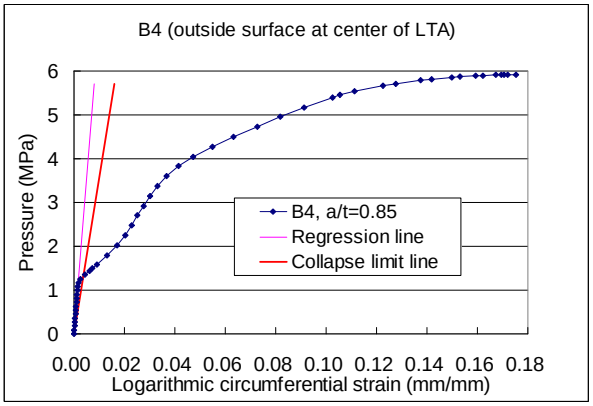

(d) B-4

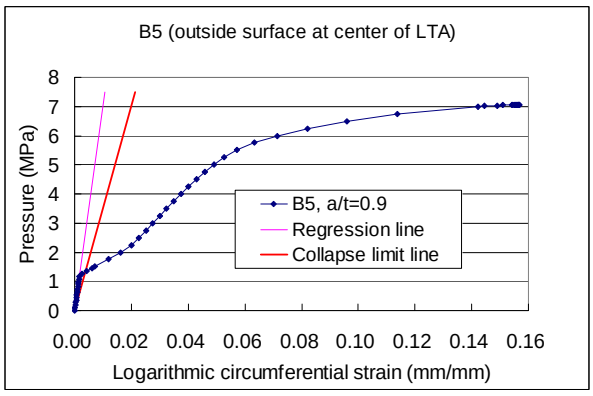

(e) B-5

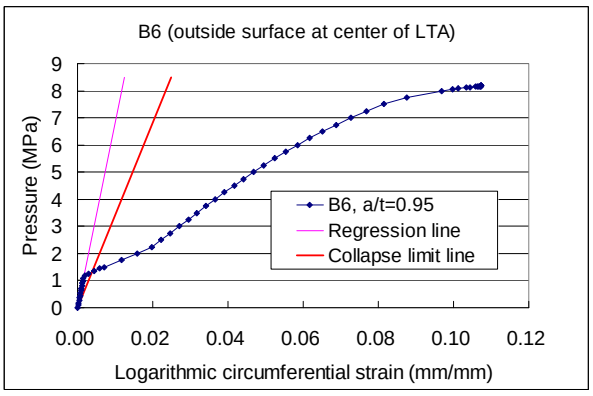

(f) B-6

Fig. 6 Strain history at center of LTA of FE model B

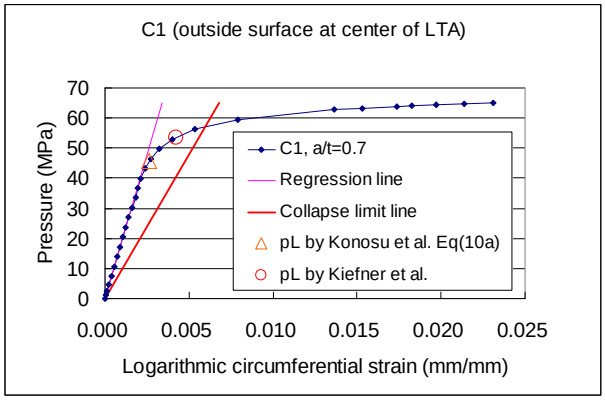

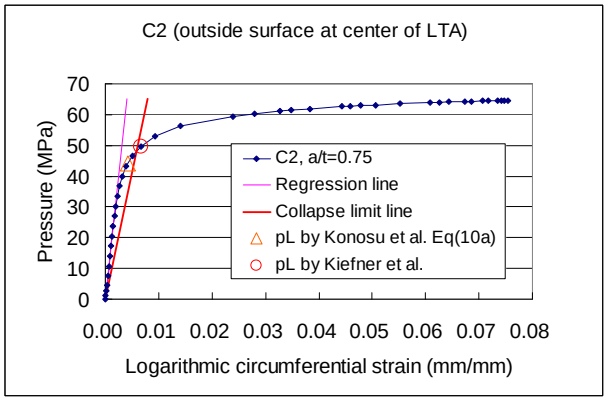

(a) C-1 (b) C-2

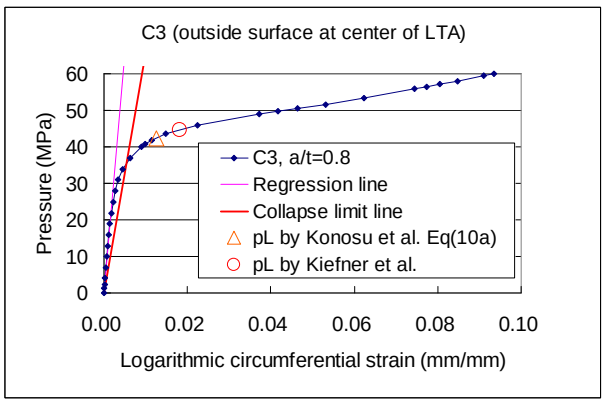

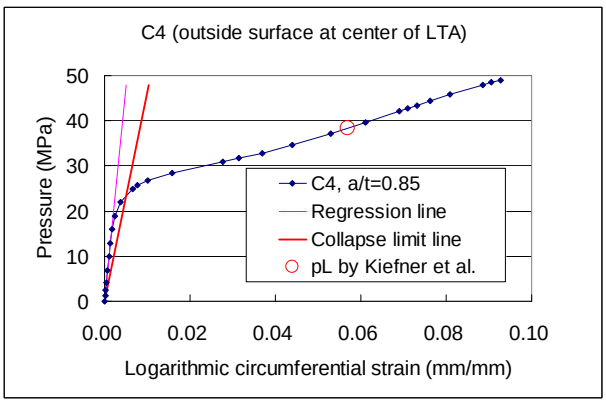

(c) C-3 (d) C-4

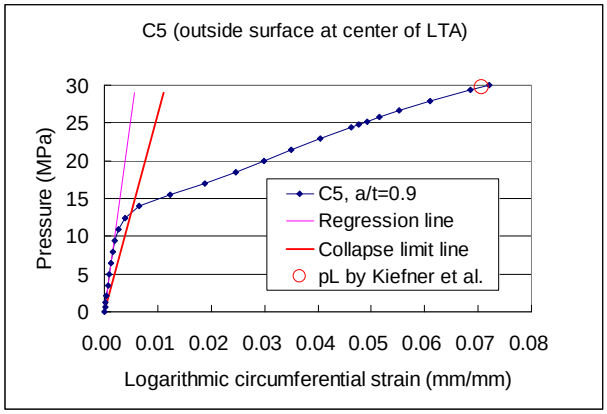

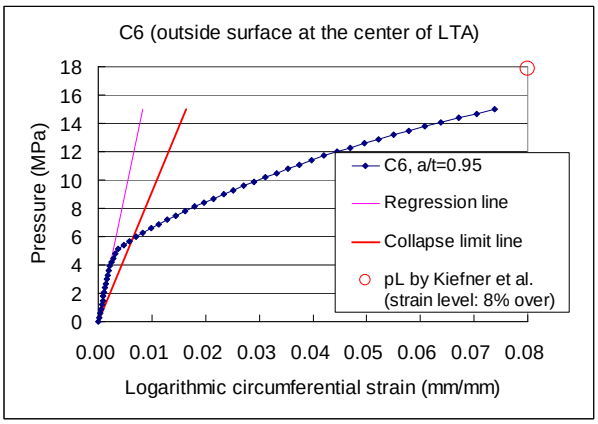

(e) C-5 (f) C-6

Fig. 7 Strain history at center of LTA of FE model C

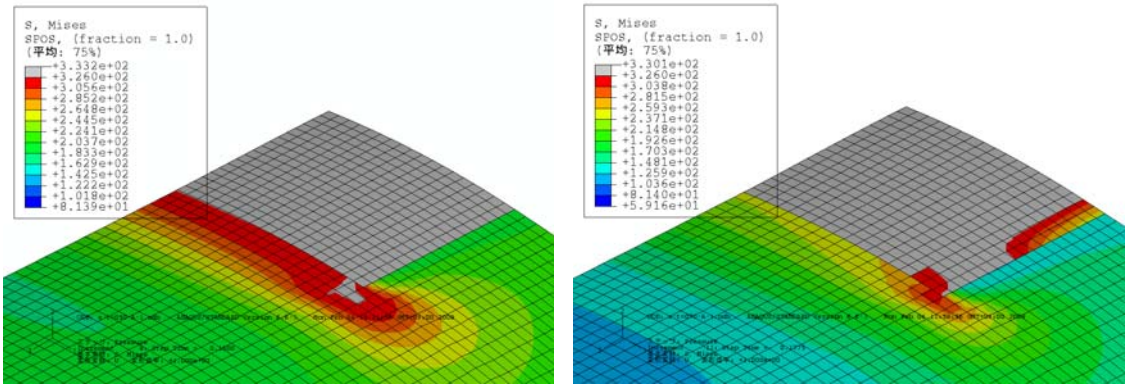

(a) A-1 (P = 4.80MPa) (b) A-2 (P = 5.33MPa)

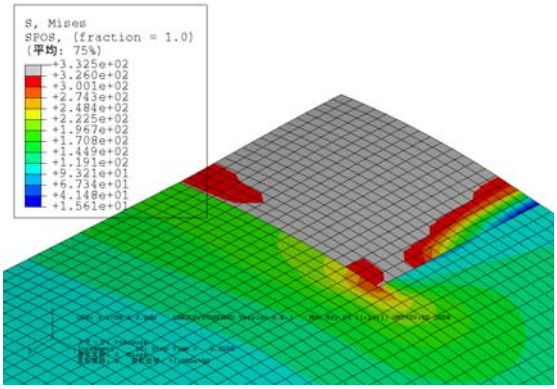

(c) A-3 (P = 6.00MPa)

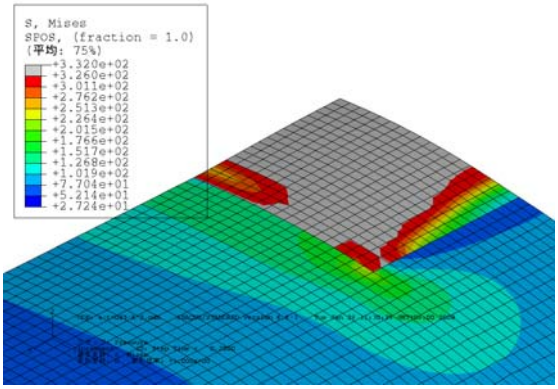

(d) A-4 (P = 6.00MPa)

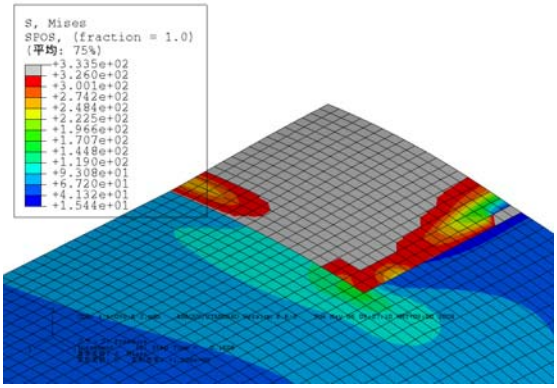

(e) A-5 (P = 6.43MPa)

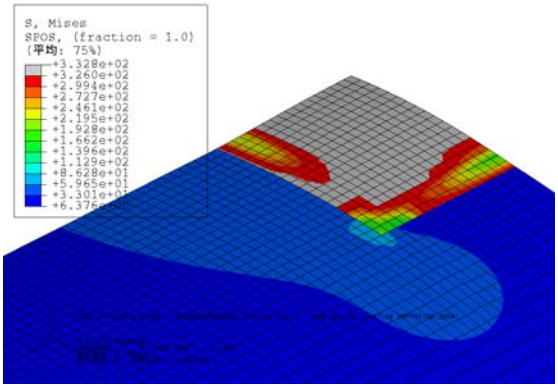

(f) A-6 (P = 6.10MPa)

Fig. 8 Mises stress on outside surface around LTA of Model A at near TES load

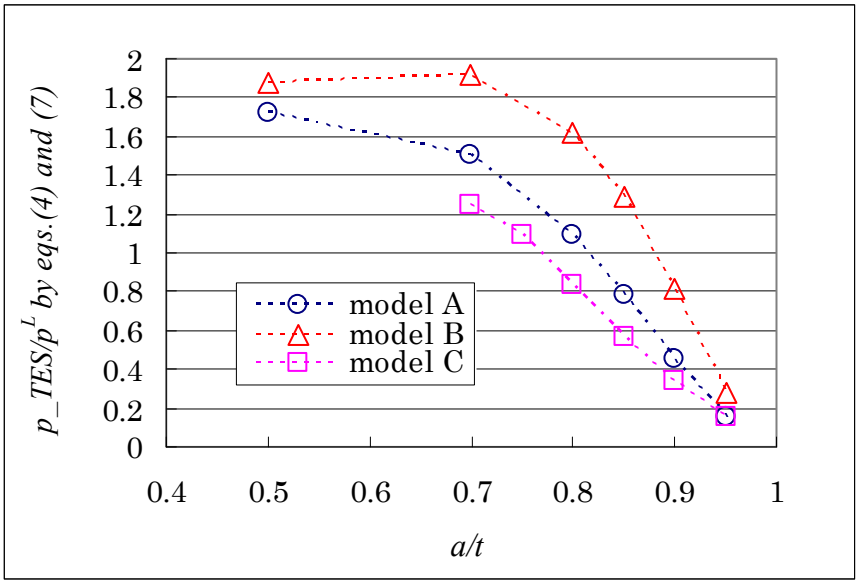

Fig. 9 The ratio of p_TES to p^L by Eqs.(4) and (7) on the collapsed load

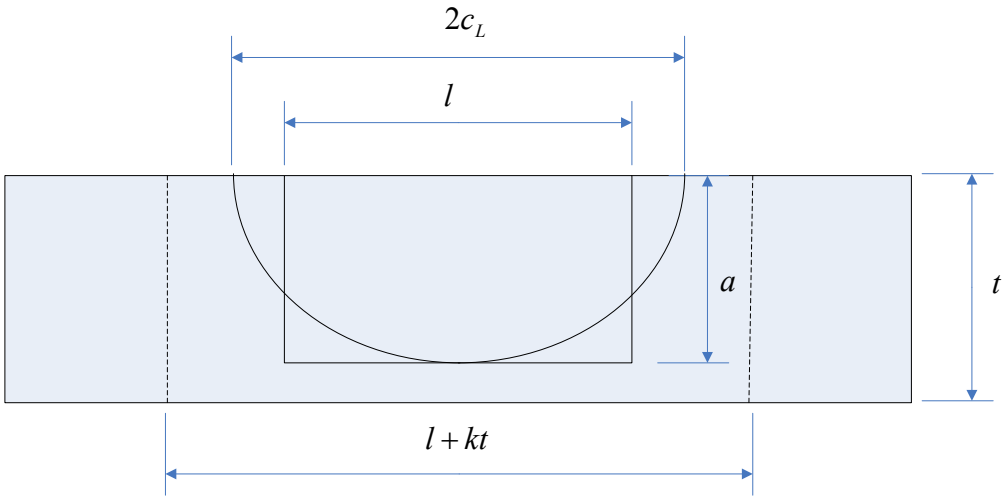

Fig. 10 Effective flaw area and effective cross section proposed here

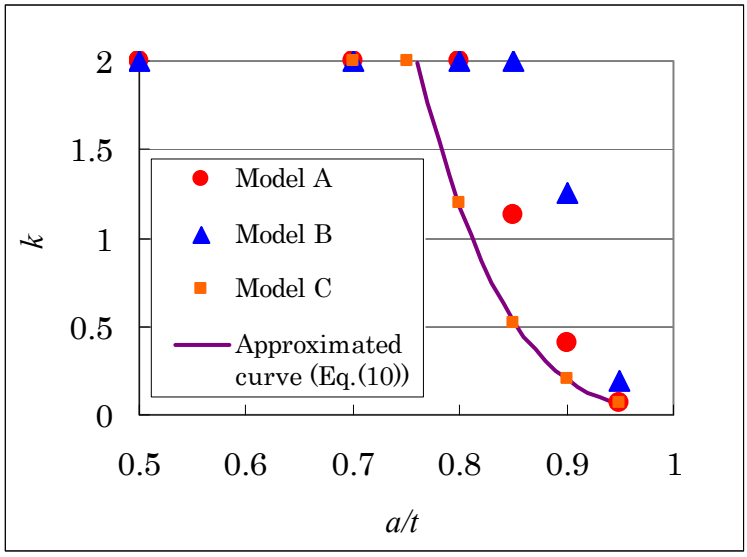

Fig. 11 The value of k where p^L becomes to p_TES

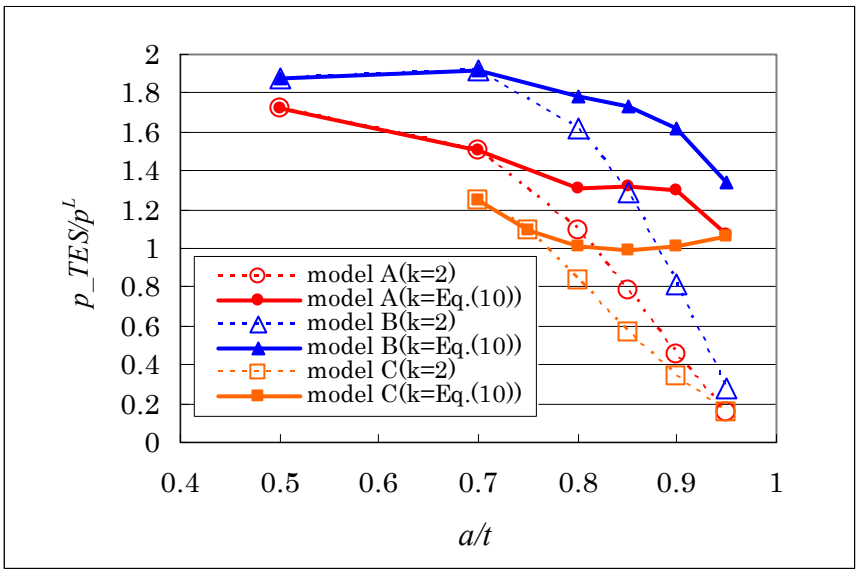

Fig. 12 The ratio of collapsed load to the collapsed load by FEM

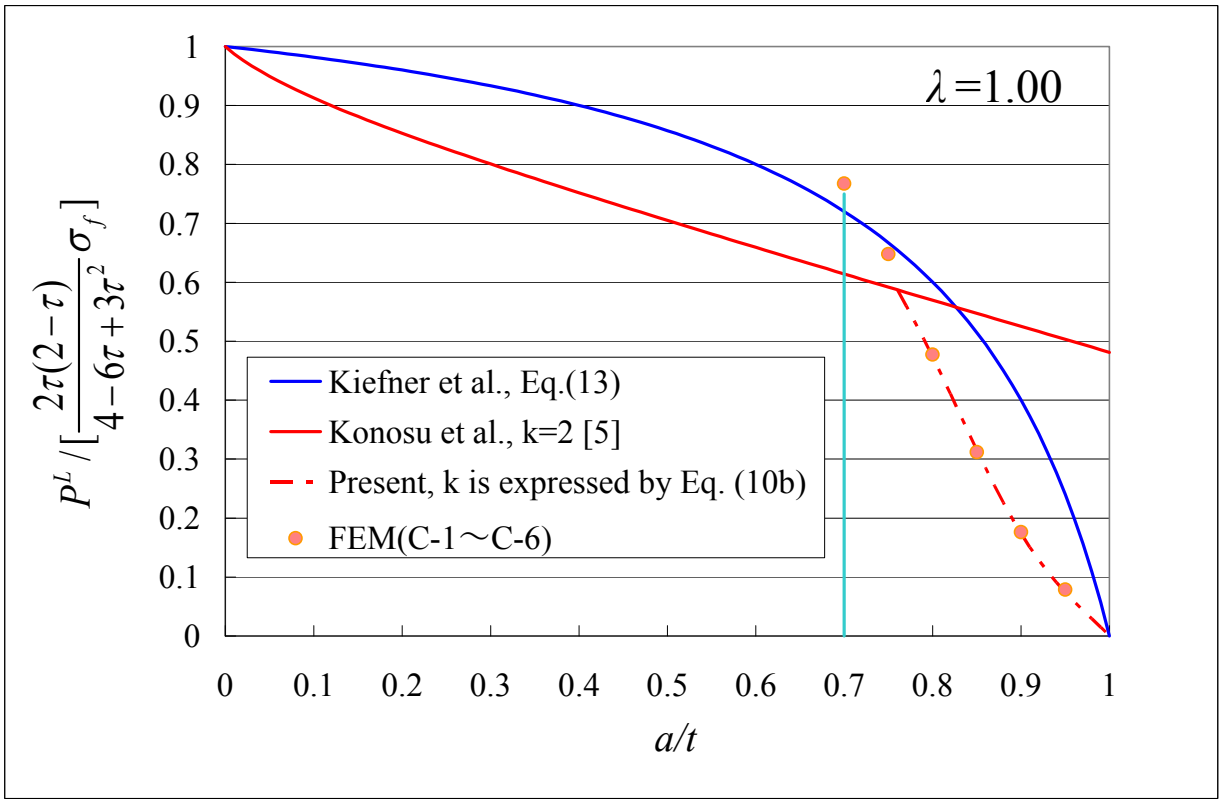

Fig. 13 The dependence of flaw depth to thickness ratio a/t on p^L / p_0^L for λ=1.0

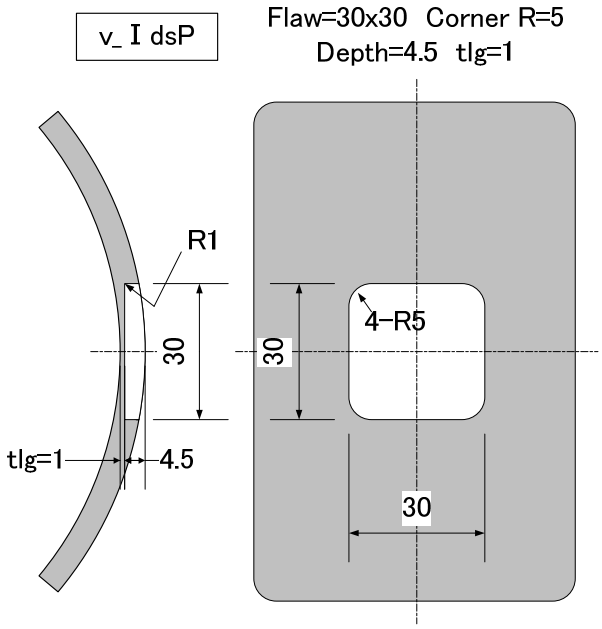

Fig. 14 Flaw configuration of experimental test

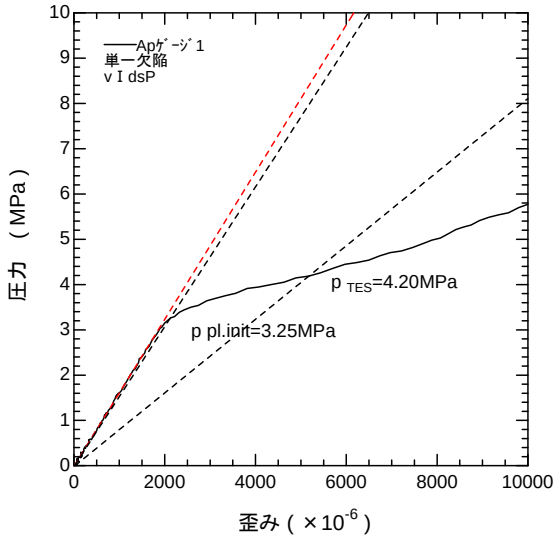

Fig. 15 Strain history at center of LTA of experimental test

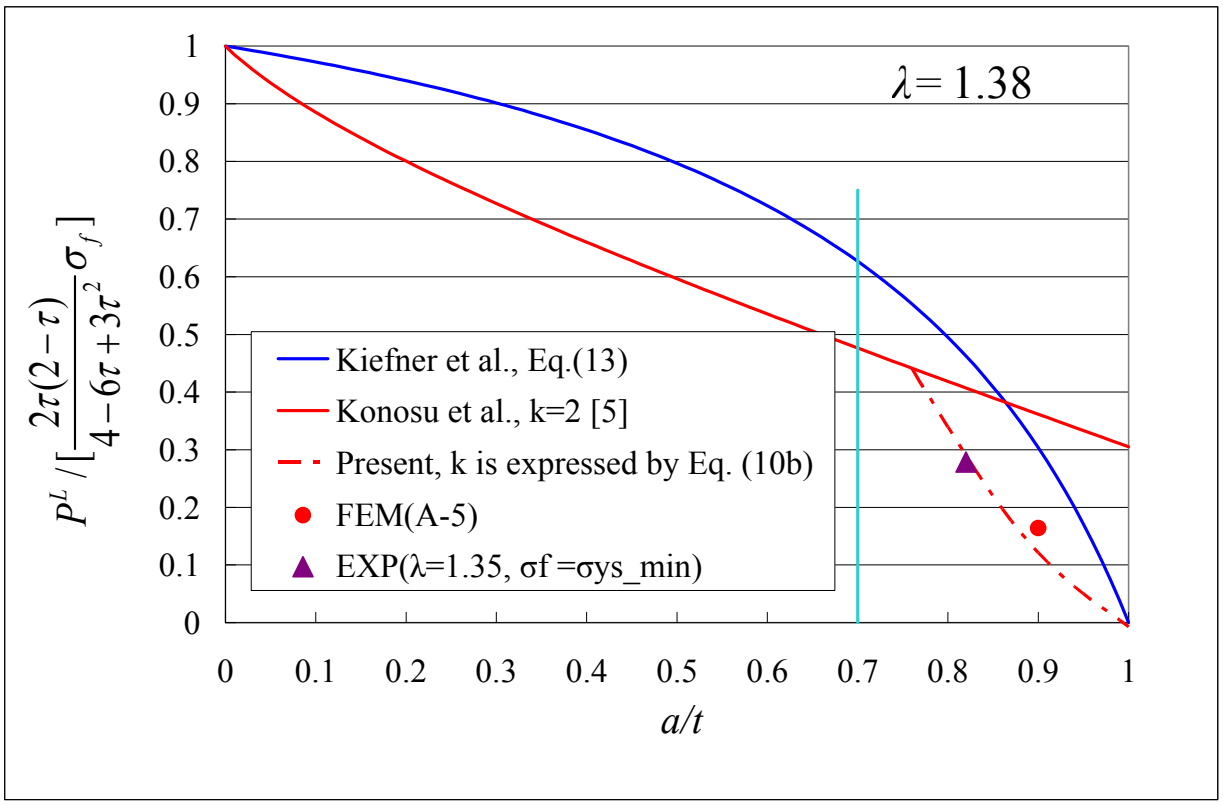

Fig. 16 The dependence of flaw depth to thickness ratio a/t on p^L / p_0^L for λ=1.4